The method described above makes it possible to efficiently evaluate the use of a given fiber composite at the design stage. This is done by performing calculations for different combinations of fibers with known characteristics. Here, the criterion of efficiency of the composite is the average density of the material obtained with the calculated optimum values of the controllable process parameters. The machine time required to optimize one variant on a BESM-6 computer is 18-20 sec.

LITERATURE CITED

1. S. M. Katz, High-Temperature Thermal-Insulating Materials [Russian translation], Moscow (1981).
2. E. N. Bershev, A. I. Kurilenko, V. V. Kuritsyna, and G. P. Smirnov, Production of Nonfabric Materials [in Russian], Moscow (1982).
3. O. A. Forges and S. G. Mason, "Hydrodynamic behavior of fibers in paper production," in: Basic Principles of Fibers Used in Paper Production, Moscow (1962), pp. 458-488.
4. D. J. Green and F. F. Lange, "Micromechanical model for fibrous ceramic bodies," J. Am. Ceram. Soc., 65, No. 3, 138-141 (1982).
5. A. I. Toropov and R. I. Nepershin, "Evaluating the stiffness and tensile strength of high-porosity fibrous materials," Mashinovedenie, No. 2, 51-56 (1987).
6. G. N. Dul'nev and Yu. P. Zarichnyak, Thermal Conductivity of Mixtures and Composites [in Russian], Leningrad (1971).
7. V. F. Kut'inov, "Design of adhesive compounds," in: Design, Development, and Testing of Structures Made of Composites [in Russian], Vol. 7, Moscow (1979), pp. 14-29.
8. E. Ya. Litovskii, S. L. Bondarenko, Yu. A. Polonskii, and N. I. Ganichev, "Effect of fiber diameter on the effective thermal conductivity of refractory insulation," Teplofiz. Vys. Temp., 17, No. 5, 997-1000 (1979).
9. R. I. Nepershin and V. V. Klimenov, "Computer optimization of a composite universal shaft with respect to cost and weight," Mekh. Kompozitn. Mater., No. 4, 690-695 (1986).

MODEL OF COMPOSITE SHALLOW SHELLS AND PLATES FOR SOLVING PROBLEMS OF STATICS, DYNAMICS, AND CONTACT INTERACTION

V. K. Prisyazhnyuk and V. G. Piskunov

UDC 539.3.624.074:624.073

Several studies [1-4, etc.] have been devoted to the design of anisotropic laminated shells and plates in accordance with the three-dimensional theory of elasticity for certain special cases permitting separation of variables. Effective use has been made of two-dimensional models of varying degrees of refinement for plates and shells in the case of more complicated boundary conditions [4-12]. These models make it possible to evaluate the stress—strain state of composite structures both at the macroscopic level — when the properties of the composite are averaged and a macroscopic homogeneous medium is examined — and at the microscopic level, i.e., directly for each phase of a heterogeneous system. Here, the possibilities for the study of composites at the microlevel are expanded by the use of variants of theories in which the order and number of resolvent equations are independent of the number of layers and the ratio of the physico-geometric parameters [6-11].

The investigation [9] constructed a theory of this type for laminated composite shallow shells and plates of orthotropic materials in which the principal directions of orthotropy coincided with the coordinate axes of the shell. Here, we generalize this theory to the case of laminated shallow shells made of anisotropic layers. The layers have one plane of elastic symmetry equidistant from the external surfaces and the surfaces of contact (interfaces) of the layers. As in [9], we will consider transverse shear and compression, tangential and normal forces of inertia, and geometric nonlinearity. In contrast to the well-known approaches taken in [6, 7], where these hypotheses were adopted a priori (independently of the physical features of the problem being examined), our approach considers these features when the assumptions are made. This is an important distinction in the design of composite structures characterized by pronounced anisotropy.

Kiev Highway Institute.

Translated from Mekhanika Kompozitnykh Materialov, No. 6, pp. 1014-1021, November-December, 1987. Original article submitted March 2, 1987.

1. To reduce the three-dimensional problem to a two-dimensional problem, we introduce the following kinematic hypotheses:

$$u_i^{(k)}(X,\tau)=u_i-w_{,i}z-\chi_{p,i}\psi_{pik}^{(j)}-\chi_{t,i}\psi_{tk};$$
$$u_3^{(k)}(X,\tau)=w+\chi_s\varphi_{sk}\quad (i=j=1,2;\ p=1,2,8,9;\ t=3\ldots 7;\ s=1\ldots 7), \tag{1.1}$$

in contrast to [9], where hypotheses are adopted for transverse shear and compression, as well as (independently) for transverse normal stresses. Here and below, it is assumed that summation is performed over the indices i, j, p, s, and t; no summation is performed over k, r, or m; $X = \{x_1, x_2, z\}$, $x = \{x_1, x_2\}$ is an orthogonal coordinate system; τ is time. Differentiation is denoted by a comma at the subscript level.

The components of the displacement vector (1.1) include: a system of independent unknown functions of the coordinate surface and time u_i, w, χ_s ($i = 1, 2$; $s = 1, 2, 3$); the prescribed functions χ_t ($t = 4\ldots9$) determined by the complete vector of the external dynamic load on the upper ($z = a_0$) $\mathbf{q}^+ = q_s^+(x, \tau)$ and lower ($z = a_r$) $\mathbf{q}^- = q_s^-(x, \tau)$ ($s = 1, 2, 3$) surfaces of the shell in the form

$$\chi_4(x,\tau)=q_{i,i}^-;\quad \chi_5(x,\tau)=q_{i,i}^-;\quad \chi_6(x,\tau)=q_3^+;$$
$$\chi_7(x,\tau)=q_3^-;\quad \chi_{8,i}(x,\tau)=q_i^+;\quad \chi_{9,i}(x,\tau)=q_i^-; \tag{1.2}$$

a system of prescribed functions of the normal z — the laws governing the change in the displacement vector over the thickness of the packet of layers. They were obtained in a solution of the problem in a first approximation (on the basis of the Kirchhoff–Love hypotheses) and satisfy the layer contact conditions, i.e., at $z = a_{k-1}$ $u_s^{(k-1)} = u_s^{(k)}$; $\sigma_{s3}^{(k-1)} = \sigma_{s3}^{(k)}$ ($s = 1, 2, 3$). They also satisfy the conditions on the external surfaces of the shell, i.e., at $z = a_0$ $\sigma_{s3}^{(1)} = -q_s^+$; at $z = a_n$ $\sigma_{s3}^{(n)} = q_s^-$. Finally, they satisfy the conditions at the level of the plane of reference, i.e., at $z = 0$ ($k = m$) $u_i^{(m)}(x, 0, \tau) = u_i(x, \tau)$; $u_3^{(m)}(x, 0, \tau) = w(x, \tau)$. Here, no distinctions are made in describing layers of different thicknesses and stiffnesses. Also, the model considers both constant physicomechanical characteristics and those which vary over the thickness of the layer. The model is thus universal in regard to the structure of the shell.

Since the form of the distribution functions over the packet thickness is rather cumbersome, as an example we will present only the relations for $\psi_{11k}^{(1)}(z)$:

$$\psi_{11k}^{(1)}(z)=\int_0^z(\varphi_{1k}-\alpha_{11k}^{(1)})dz;\quad \varphi_{1k}(z)=\int_0^z\beta_{1k}dz;$$

$$\alpha_{11k}^{(1)}(z)=a_{45k}f_{12k}+a_{55k}f_{11k};\quad \beta_{1k}(z)=-(a_{13k}B_{11k}+a_{23k}B_{12k}+a_{36k}B_{16k})z;\quad f_{11k}(z)=f^*_{11k}-D_{11}f^*_{16k}K_{16}^{-1};$$

$$f_{12k}(z)=f^*_{12k}-D_{16}f^*_{16k}K_{16}^{-1};\quad f^*_{11k}(z)=\int_{a_0}^z B_{11k}zdz;$$

$$f^*_{12k}(z)=\int_{a_0}^s B_{16k}zdz;\quad f^*_{16k}(z)=\int_{a_0}^z B_{16k}dz;\quad D_{11}=\int_{a_0}^{a_k} B_{11k}zdz; \tag{1.3}$$

$$D_{16}=\int_{a_0}^{a_n} B_{16k}zdz;\quad K_{16}=\int_{a_0}^{a_n} B_{16k}dz;$$

$$B_{11k}=(a_{22k}a_{66k}-a_{26k}^2)/\Delta;\quad B_{12k}=(a_{16k}a_{26k}-a_{12k}a_{66k})/\Delta;$$
$$B_{16k}=(a_{12k}a_{26k}-a_{16k}a_{22k})/\Delta;\quad \Delta=a_{11k}B_{11k}+a_{12k}B_{12k}+a_{16k}B_{16k},$$

where $a_{11k}\ldots a_{66k}$ are elastic constants for the anisotropic body [6].

It follows from (1.3) that the law governing the change in the components of the displacement vector over the thickness of the packet is independent of the choice of reference plane. Here, the tangential displacements are approximated over the shell thickness by a fifth-degree polynomial, while the normal displacements are approximated by a fourth-degree polynomial (cubic and square parabolas were used in [4, 7], respectively).

The physical interpretation of the terms in (1.1) is determined by the functions of the normal z. For example, the terms which include the functions $\varphi_{pk}(z)$ (p = 1, 2, 4...7) account for transverse static compression, while the terms including $\varphi_{3k}(z)$ account for dynamic compression. In fact, for layers which are not compressed along the normal ($E_{3k} = \infty$) we have $\varphi_{pk}(z) = 0$ (p = 1...7); then

$$u_i^{(k)}(X,\tau) = u_i - w_{,i}z - \chi_{p,i}\psi_{pik}^{(j)};\quad u_3^{(k)}(X,\tau) = w \quad (i=j=1,2;\quad p=1,2,8,9). \tag{1.4}$$

The above kinematic model considers only transverse shear and is analogous to the model constructed in [10] for problems of the statics of homogeneous plates. At $G_{i3k} = \infty$, we have $\varphi_{pik}^{(j)}(z) = 0$ and we arrive at a special case — the displacements of the classical theory [4, 6]: $u_i^{(k)}(X, \tau) = u_i - w_{,i}z$; $u_3^{(k)}(X, \tau) = w$. Thus, the functions $\chi_1(x, \tau)$ and $\chi_2(x, \tau)$ simultaneously consider both shear and transverse compression, while $\chi_3(x, \tau)$ considers dynamic compression and, as in [8, 9], it accounts for the change in the length of the normal from inertial forces in the transverse direction. The remaining terms, including the functions $\chi_t(x, \tau)$ (t = 4...9), are determined by the external load (1.2). Thus, they account for shear and compression resulting directly from this load. This fact is important in the solution of contact problems [12].

As with the models described in [8-10], one feature of the proposed model is that Eqs. (1.1) and (1.4) contain similar terms accounting for the states of pure bending, shear, and compression. These terms are absent from the models described in [6, 7]. Their inclusion here makes it possible to efficiently realize the model through approximate methods, by resorting to an independent but analogous approximation of the displacement-vector components for the different states. The inclusion of the terms in the present model also makes it possible to generalize the methods and results obtained from the solution of the given problems in the classical theory to the nonclassical theory being used here. In particular, proceeding on this basis, we can efficiently realize the present model by the finite elements method.

To obtain the components of the strain tensor, we use geometric relations in which we consider geometric nonlinearity in the direction of the normal z [6]:

$$\begin{gathered}2e_{ij}^{(k)} = u_{i,j}^{(k)} + u_{j,i}^{(k)} + 2k_{ij}u_3^{(k)} + u_{3,i}^{(k)}u_{3,j}^{(k)};\\ 2e_{33}^{(k)} = 2u_{3,3}^{(k)} + [u_{3,3}^{(k)}]^2;\quad 2e_{i3}^{(k)} = u_{i,3}^{(k)} + u_{3,i}^{(k)} + u_{3,i}^{(k)}u_{3,3}^{(k)}.\end{gathered} \tag{1.5}$$

Assumptions made in regard to the smallness of the strains allow us to write [11]

$$u_{3,i}^{(k)}u_{3,j}^{(k)} \approx w_{,i}w_{,j};\quad [u_{3,3}^{(k)}]^2 \approx 0;\quad u_{3,i}^{(k)}u_{3,3}^{(k)} \approx 0.$$

Considering this and ignoring terms on the order of $k_{ij}z$ with the substitution of (1.1) into (1.5), we obtain

$$\begin{gathered}e_{11}^{(k)} = \varepsilon_{11} + \varkappa_{11}z + \varkappa_{11}^{(p)}\psi_{p1k}^{(1)} + \varkappa_{11}^{(t)}\psi_{tk};\quad e_{22}^{(k)} \rightleftarrows e_{11}^{(k)};\\ 2e_{12}^{(k)} = 2\varepsilon_{12} + 2\varkappa_{12}z + \varkappa_{11}^{(p)}\psi_{p1k}^{(2)} + \varkappa_{12}^{(p)}(\psi_{p1k}^{(1)} + \psi_{p2k}^{(2)}) +\\ + \varkappa_{22}^{(p)}\psi_{p2k}^{(1)} + 2\varkappa_{12}^{(t)}\psi_{tk};\\ e_{33}^{(k)} = \chi_g\beta_{gk};\quad 2e_{i3}^{(k)} = \chi_{p,i}\alpha_{pik}^{(j)};\quad \varepsilon_{ij} = 0{,}5(u_{i,j} + u_{j,i} + k_{ij}w + w_{,i}w_{,j});\\ \varkappa_{ij} = -w_{,ij};\quad \varkappa_{ij}^{(s)} = -\chi_{s,ij}\\ (i,j=1,2;\ p=1,2,8,9;\ t=3\ldots7;\ g=1\ldots7;\ s=1\ldots9).\end{gathered} \tag{1.6}$$

Using Hooke's law for an anisotropic body [4, 6], as which we regard the layer k, and using (1.6), we find the components of the stress tensor

$$\sigma_{ij}^{(k)} = A_{ijst}^{(k)}e_{st}^{(k)}\quad (i,j,s,t=1,2,3). \tag{1.7}$$

Thus, we have obtained all of the components of the stress and strain tensors forming the model of an anisotropic piecewise-nonuniform shallow shell having an arbitrary structure over the thickness. The model differs from the well-known models in [4-12] in the completeness of the allowance for transverse shear and compression and geometric nonlinearity and the completeness of the connection with the elastic constants of the anisotropic material. As in [8, 9], by its physical nature the present model is a dynamic model, accounting for the effect of transverse compression from inertial forces.

The transition to special cases is made by adopting assumptions regarding the physico-mechanical properties of the layers.

2. To obtain the equations of motion, we use the Hamilton–Ostrograd variational principle [5, 8]. In accordance with the latter, the action integral $I=\int_{\tau_0}^{\tau_1}(T-U-\Pi)d\tau$ takes a steady value only for true motion, i.e., $\delta I = 0$. Here, T is the kinetic energy of the system; U is the potential energy associated with deformation; Π is the potential of the external forces.

Use of the variational principle "...naturally solves the problem of generalized internal forces corresponding to chosen hypotheses and the problem of consistent boundary conditions" [5].

If we take the variation of kinetic energy

$$\delta T=-\iint_S\left(\int_{a_0}^{a_n}\rho_k\ddot{u}_s^{(k)}\delta u_s^{(k)}dz\right)dS \quad (s=1,2,3),$$

the variation of strain potential energy

$$\delta U=\iiint_V\sigma_{st}^{(k)}\delta e_{st}^{(k)}dV \quad (s,t=1,2,3),$$

and the variation of the external load and contour forces

$$\delta\Pi=\iint_S[q_s^+\delta u_s^{(1)}(a_0)+q_s^-\delta u_s^{(n)}(a_n)]dS+\int_\Gamma(\sigma^{*(k)}_{hh}\delta u_h^{(k)}+\sigma^{*(k)}_{hl}\delta u_l^{(k)}+\sigma^{*(k)}_{h3}\delta u_3^{(k)})d\Gamma \quad (s=1,2,3;\ h,l=1,2)$$

and we insert the expressions for the components of the displacement vector (1.1) and strain tensor (1.3), by then varying the unknown independent functions u_i, w, and χ_s ($i = 1, 2$; $s = 1, 2, 3$) we obtain a system of resolvent equations of motion in forces

$$\begin{aligned}
&\mathbf{N}_{ij,j}-\mathbf{U}_i+\mathbf{q}_i=0 \quad (i,j=1,2);\\
&\mathbf{M}_{ij,ij}+(\mathbf{N}_{ij}\mathbf{w}_{,i})_{,j}-\mathbf{k}_{ij}\mathbf{N}_{ij}-\mathbf{U}_{ii,q}-\mathbf{U}_3+\mathbf{q}_3=0;\\
&\mathbf{M}_{ij,ij}^{(p)}+\mathbf{Q}_{i,i}^{(p)}-\mathbf{Q}_3^{(p)}-\mathbf{U}_{ii,g}^{(p)}+\mathbf{q}_3^{(p)}=0 \quad (p=1,2);\\
&\mathbf{M}_{ij,ij}^{(3)}-\mathbf{Q}_3^{(3)}-\mathbf{U}_{ii,g}^{(3)}+\mathbf{q}_3^{(3)}=0 \quad (g=i)
\end{aligned} \tag{2.1}$$

and the corresponding boundary conditions

$$\begin{aligned}
&(N_{hh}-N^*_{hh})\delta u_h=0;\quad (N_{hl}-N^*_{hl})\delta u_l=0;\quad (M_{hh}-M^*_{hh})\delta w_{,h}=0;\\
&(M_{hh,h}+2M_{hl,l}+N_{hh}w_{,h}+N_{hl}w_{,l}-U_{hh}+q_h-R^*_h)\delta w=0;\\
&[M_{hh,h}^{(p)}+2M_{hl,l}^{(p)}+Q_h^{(p)}-U_{hh}^{(p)}+q_h^{(p)}-R^{*(p)}_h]\delta\chi_p=0 \quad (p=1,2);\\
&[M_{hh,h}^{(3)}+2M_{hl,l}^{(3)}-U_{hh}^{(3)}+q_h^{(3)}-R^{*(3)}_h]\delta\chi_3=0;\\
&[M_{hh}^{(s)}-M^{*(s)}_{hh}]\delta\chi_{s,h}=0 \quad (s=1,2,3;\ h,l=1,2).
\end{aligned} \tag{2.2}$$

In (2.1) and (2.2), we used the following notation for the external loads:

$$\begin{gathered}
q_i=q_i^++q_i^-;\quad q_3=q_3^++q_3^-+a_0q_{i,i}^++a_nq_{i,i}^-;\\
q_3^{(p)}=\varphi_{p1}(a_0)q_3^++\varphi_{pn}(a_n)q_3^-+\psi_{pi1}^{(j)}(a_0)q_{i,i}^++\psi_{pin}^{(j)}(a_n)q_{i,i}^-;\\
q_3^{(3)}=\varphi_{31}(a_0)q_3^++\varphi_{3n}(a_n)q_3^-+\psi_{31}(a_0)q_{i,i}^++\psi_{3n}(a_n)q_{i,i}^-;\\
q_h=q_h^+a_0+q_h^-a_n;\quad q_h^{(p)}=\psi_{p11}^{(h)}(a_0)q_h^++\psi_{p1n}^{(h)}(a_n)q_h^- \quad (p=1,2);\\
q_h^{(3)}=\psi_{31}(a_0)q_h^++\psi_{3n}(a_n)q_h^-;
\end{gathered}$$

while the notation for the contour forces is

$$R^*_h = Q^*_h + M^*_{hl,l}; \quad R^{*(s)}_h = Q^{*(s)}_h + M^{*(s)}_{hl,l} \qquad (s = 1, 2, 3),$$

where h is the normal and l is a tangent to the contour Γ.

Equations (2.1) and the corresponding boundary conditions contain generalized forces and inertia forces familiar from the classical theory of shells based on the Kirchhoff–Love hypotheses. They also contain higher-order generalized and inertial forces. As in [4, 5, 7-10], this allows us to obtain complete agreement between the adopted kinematic model (1.1) and the system of internal forces. This situation is in contrast to [6, 11, 12], where such forces were not introduced. We will present only some of them as an example:

$$M_{11}^{(1)} = M_{1111}^{(1)} + M_{1211}^{(2)}; \qquad Q_1^{(1)} = Q_{111}^{(1)} + Q_{211}^{(2)}; \qquad U_{11}^{(1)} = U_{1111}^{(1)} + U_{2211}^{(2)};$$

$$M_{1111}^{(1)} = \int_{a_0}^{a_n} \sigma_{11}{}^{(k)}\psi_{11}{}^{(1)}dz; \quad M_{1211}^{(2)} = \int_{a_0}^{a_n} \sigma_{12}{}^{(k)}\psi_{11k}{}^{(2)}dz;$$

$$Q_3{}^{(1)} = \int_{a_0}^{a_n} \sigma_{33}{}^{(k)}\beta_{1k}dz; \quad Q_{111}{}^{(1)} = \int_{a_0}^{a_n} \sigma_{13}{}^{(k)}\alpha_{11k}{}^{(1)}dz;$$

$$Q_{211}{}^{(2)} = \int_{a_0}^{a_n} \sigma_{23}{}^{(k)}\alpha_{11k}{}^{(2)}dz; \quad U_3{}^{(1)} = \int_{a_0}^{a_n} \rho_k \ddot{u}_3{}^{(k)}\varphi_{1k}dz;$$

$$U_{1111}^{(1)} = \int_{a_0}^{a_n} \rho_k \ddot{u}_1{}^{(k)}\psi_{11k}{}^{(1)}dz; \quad U_{2211}^{(2)} = \int_{a_0}^{a_n} \rho_k \ddot{u}_2{}^{(k)}\psi_{11k}{}^{(2)}dz.$$

The overall order of system of resolvent equations (2.1), written in displacements, is 20 and is in full accord with the number of boundary conditions (2.2) — ten for each side of the shell. It is possible to use boundary conditions (2.2) to model different types of constraints on the contour of the shell. Here, by analogy with [8, 9], we distinguish two groups of conditions. The first group models external (contour) constraints imposed on the contour of a two-dimensional region of the coordinate surface of the shell ($z = 0$) and determines its fastening as a whole (simple support, fixed ends, etc.). The second group models constraints which prevent mutual displacement of points on the ends of the contour over its thickness ($z \neq 0$). These are called internal or end constraints. Combining the two groups of conditions (2.2), we are able to design anisotropic shells and plates with different structural features on the contour.

3. Let us examine some examples illustrating the ability of the proposed model to reflect the three-dimensional character of the stress-strain state of multilaminate shells and plates.

Example 1. The bending of a square plate, made of a multilaminate composite (three and nine layers), under a sinusoidal load. Results of the three-dimensional solution of this problem, with Navier-type boundary conditions, are given in [3], which also describes all of the physico-geometric parameters of the plate. In the theory being proposed here for nonuniform shells and plates, the square plate is adequately modeled with hinged support about the contour and membranes which are flexible outside the end plane but rigid within this plane. The material of each layer is a unidirectionally reinforced composite with the parameters $E_L = 172 \cdot 10^3$ MN/m²; $E_T = 6.9 \cdot 10^3$ MN/m²; $\nu_{LT} = \nu_{TT} = 0.25$; $G_{LT} = 3.25 \cdot 10^3$ MN/m²; $G_{TT} = 1.38 \cdot 10^3$ MN/m² where L corresponds to the direction along the fibers and T to the direction across the fibers.

The above problem was solved with the proposed model by means of double trigonometric series and was compared with the three-dimensional solution and the results of the classical theory of plates (CTP) reported in [3]. It is evident from Table 1 that the proposed model (II) makes it possible to obtain reliable results for plates of hybrid composites with an arbitrary number of layers and the ratio $S = a/h \_ 4$. If $S < 4$, then the divergence from the three-dimensional solution (I) is greater than the error of the practical calculations ($\Delta > 5\%$). This can be attributed to the use of two-dimensional (albeit refined) model in the calculations. Even for thin laminated anisotropic plates with $S = 20$, the CTP leads to displacement errors greater than the permissible value ($\Delta > 10\%$). However, the Kirchhoff hypothesis is valid at $S \geq 5$ for uniform isotropic plates.

TABLE 1. Comparison of Dimensionless Values of the Stresses $(\bar{\sigma}_{11}, \bar{\sigma}_{22}, \bar{\sigma}_{12}) = (\sigma_{11}, \sigma_{22}, \sigma_{12})/q_0S^2$, $(\bar{\sigma}_{13}, \bar{\sigma}_{23}) = (\sigma_{13}, \sigma_{23})/q_0S$ and Normal Displacements $\bar{u}_3^{(k)} = \pi^4 Qu_3^{(k)}/12q_0hS^4$, $Q = 4\cdot G_{LT} + [E_L + E_T(1 + 2\nu_{TT})]/(1 - \nu_{LT}\nu_{TT})$ Obtained on the Basis of the Three-Dimensional Solution (I), the Proposed Model (II), and the CTP

$S=a/h$	$\bar{\sigma}_{11}$		$\bar{\sigma}_{12}$		$\bar{\sigma}_{23}$		$\bar{u}_3$	
	$a/2,\ a/2,\ \pm 0.5$		$0,\ 0,\ \pm 0.5$		$a/2,\ 0,\ 0$		$a/2,\ a/2,\ 0$	
	I	II	I	II	I	II	I	II
	Three-layer plate							
2	1.388 −0.912	1.859 −1.052	−0.0863 0.0673	−0.1172 0.0711	0.295	0.298	11.767	10.344
4	0.720 −0.684	0.729 −0.742	−0.0467 0.0458	−0.0474 0.0487	0.292	0.305	4.491	4.464
10	±0.559	0.559 −0.556	−0.0275 0.0276	−0.0276 0.0278	0.196	0.199	1.709	1.708
20	±0.543	±0.543	∓0.0230	∓0.0230	0.156	0.156	1.189	1.189
CTP	±0.539		∓0.0213		0.138		1.000	
	Nine-layer plate							
2	1.260 −0.866	1.860 −0.738	−0.0722 0.0534	−0.0952 0.0491	0.211	0.216	12.288	11.468
4	0.684 −0.649	0.725 −0.665	−0.0337 0.0328	−0.0353 0.0334	0.225	0.237	4.079	4.049
10	±0.551	±0.552	−0.0233 0.0235	−0.0234	0.226	0.229	1.512	1.511
20	±0.541	±0.541	∓0.0218	∓0.0218	0.221	0.222	1.129	1.129
CTP	±0.539		∓0.0213		0.219		1.000	

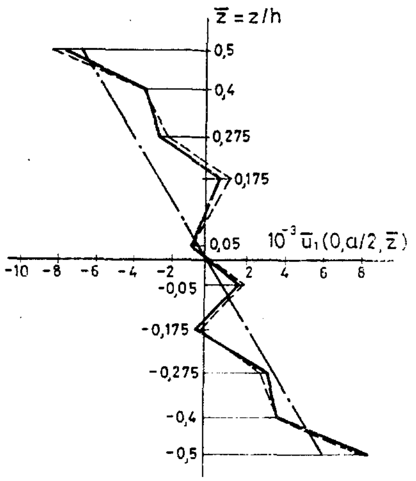

Fig. 1

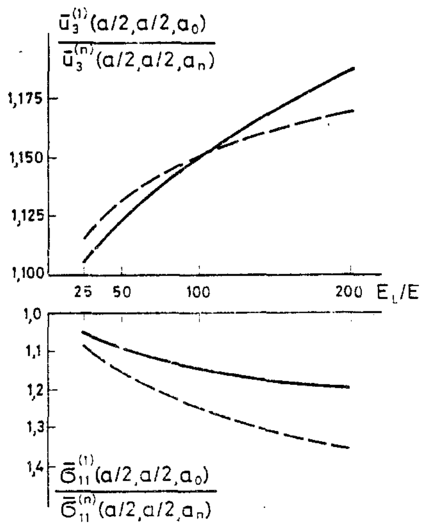

Fig. 2

Fig. 1. Laws of change in the tangential displacements over the thickness of a nine-layer plate with S = 4 and the structure [0°/90°/0°/90°/0°/90°/0°/90°/0°]. (———) three-dimensional solution; (-----) proposed solution; (—•—•—•—) solution obtained from the CTP.

Fig. 2. Change in the ratio of the maximum and minimum normal stresses $\bar{\sigma}_{11}$ and displacements u_3 in relation to the orthotropy coefficient $n_0 = E_L/E_T$ for a three-layer plate with the structure [0°/90°/0°] (———) and the nine-layer plate (-----).

The distribution law for the tangential displacements over the thickness of the nine-layer plate at S = 4 (Fig. 1) is both qualitatively and quantitatively close to the three-dimensional solution (solid line). The CTP (dot–dash line) does not reliably reflect the pattern of change in $\bar{u}_1^{(k)}(0, a/2, \bar{z}) = E_T u_1^{(k)}/q_0hS^3$ over the thickness of the plate.

We studied the effect of the orthotropy coefficient $n_0 = E_L/E_T$ on the stress–strain state of a three-layer plate (solid line in Fig. 2) and a nine-layer plate (dashed line). Both

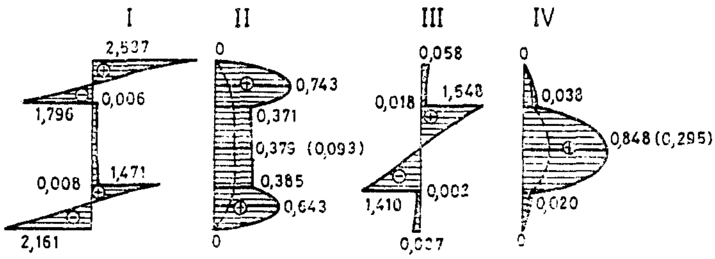

Fig. 3. Diagrams of normal and transverse shear stresses in a three-layer composite plate with the structure [0°/90°/0°].

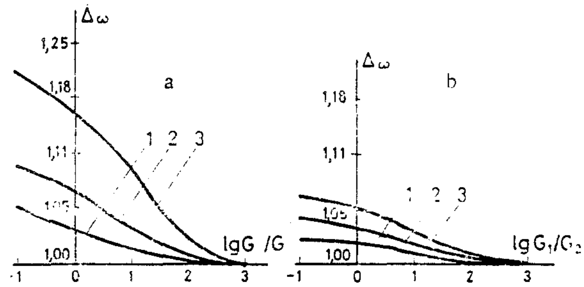

Fig. 4. Curves of the ratio of frequencies for a three-layer plate obtained in special cases of the proposed theory to frequencies found in the general case for ratios of the density of the bearing layer to the filler $\rho_1/\rho_2 = 100$ (a) and 10 (b). 1) without allowance for static compression from the Poisson effect ($\nu'_k = 0$); 2) without allowance for either static or dynamic compression ($E'_{3k} = \infty$); 3) without allowance for transverse compression or tangential inertial forces ($E'_{3k} = \infty$, $\ddot{u}_i^{(k)} = 0$).

plates were of moderate thickness, with S = 4. It was found that with an increase in the orthotropy coefficient, there was a significant difference (up to 35%) between the displacements and stresses on the loaded and free surfaces of the symmetrical plates (see Fig. 2). Use of the models in [6, 7, 10, 11] and the CTP failed to show this effect, since the laws governing the change in the normal stresses and displacements over the thicknesses of these plates are symmetrical functions.

Figure 3 shows diagrams of the normal stresses $\bar{\sigma}_{11}(a/2,\ a/2,\ \bar{z})$ (I), $\bar{\sigma}_{22}(a/2,\ a/2,\ \bar{z})$ (III) and transverse shear stresses $\bar{\sigma}_{13}(0,\ a/2,\ \bar{z})$ (II), $\bar{\sigma}_{23}(a/2,\ 0,\ \bar{z})$ (IV) for a three-layer plate in which $n_0 = 200$ and S = 4. As in [1], the transverse shear stresses were obtained by integrating the equilibrium equations

$$\sigma_{i3}^{(k)} = -\int_{a_0}^{z} \sigma_{ij,j}^{(k)}dz + \Phi_{ik} \quad (i,\ j = 1,\ 2),$$

in which $\sigma_{ij}^{(k)}$ is replaced by the refined expression (1.7). The latter considers both transverse shear strain and compressive strain.

The change in the transverse shear stresses is both qualitatively and quantitatively different from that found by the CTP (dashed line in Fig. 3) and agrees in form with the change found in [1, 3].

Example 2. Let us investigate the physicogeometric parameters at which the frequencies of transverse vibrations are affected by higher-order factors not considered by the classical theory: transverse shear strain ($G'_k \neq \infty$), rotational inertia and curvature, tangential inertial forces ($\ddot{u}_i^{(k)} \neq 0$), and static ($\nu'_k \neq 0$) and dynamic ($E'_k \neq \infty$) compression. To do this, we examine the natural vibrations of a square three-layer plate with thin external layers ($h_2/h_1 = 18$) and a high relative density ($\rho_1/\rho_2 = 100$). The material of the layers is a transversely isotropic composite. The ratio of the half-wavelengths to the overall thickness of the plate $l/h = 4$.

The curves in Fig. 4 show the ratio Δ_ω of the frequencies obtained in special cases of the proposed theory to the frequencies found in the general case. The latter coincide with the exact solution of the three-dimensional problem. In the case of a low-stiffness filler ($G_1/G_2 = 10^3$), for the structure in question we need consider only transverse shear in order to obtain agreement with the exact solution. The effect of transverse shear decreases significantly with an increase in the shear modulus of the filler ($G_1/G_2 < 10^3$). At the same time, the effect of the other higher-order factors increases, and failure to allow for them in the solution of the vibration problem for laminated composite structures will lead to errors in the calculations. The effect of dynamic compression and rotational inertia increases in the case of external layers with a high relative density (see Fig. 4a). The parameter regions in which these factors should be considered are as follows: $G_1/G_2 \leq 10$; $\rho_1/\rho_2 > 10$; $h_2/h_1 > 10$; $l/h \leq 4$.

The difference between the solution obtained without allowance for compression and tangential inertial forces and the exact solution is greatest for plates with a stiff, low-density filler (the difference is more than 15%).

LITERATURE CITED

1. A. E. Bogdanovich, "Calculation of transverse and interlayer stresses in cylindrical shells of laminated composites under compressive dynamic loads," Mekh. Kompozitn. Mater., No. 3, 455-467 (1985).
2. Ya. M. Grigorenko, A. T. Vasilenko, and N. D. Pankratova, Statics of Anisotropic Thick-Walled Shells [in Russian], Kiev (1985).
3. N. J. Pagano and S. J. Hatfield, "Elastic behavior of multilayered bidirectional composites," AIAA J., 10, No. 7, 931-933 (1972).
4. R. Christensen, Introduction to the Mechanics of Composites [Russian translation], Moscow (1982).
5. V. V. Bolotin and Yu. N. Novichkov, Mechanics of Multilayered Structures [in Russian], Moscow (1980).
6. S. A. Ambartsumyan, General Theory of Anisotropic Shells [in Russian], Moscow (1974).
7. A. O. Rasskazov, "Toward a theory of multilayered orthotropic shallow shells," Prikl. Mekh., 12, No. 11, 50-56 (1976).
8. V. G. Piskunov, "One variant of the nonclassical theory of nonuniform shallow shells and plates," Prikl. Mekh., 15, No. 11, 76-81 (1979).
9. V. G. Piskunov and V. K. Prisyazhnyuk, "Nonclassical model of multilayered shells of orthotropic composites for the solution of dynamic problems," Dokl. Akad. Nauk Ukr. SSR, Ser.A, No. 4, 43-47 (1986).
10. V. G. Piskunov, A. G. Gurtovyi, and V. S. Sipetov, "Refinement of the theory of anisotropic plates," Prikl. Mekh., 20, No. 5, 82-87 (1984).
11. A. F. Ryabov, Design of Multilaminate Shells [in Ukrainian], Kiev (1968).
12. E. I. Grigolyuk and V. M. Tolkachev, Contact Problems of the Theory of Plates and Shells [in Russian], Moscow (1980).